Fast Solution of Multi-Scale Antenna Problems for the Square Kilometre Array (SKA) Radio Telescope using the Characteristic Basis Function Method (CBFM)

Rob Maaskant [1], Raj Mittra [2], and Anton Tijhuis [3]

[1] The Netherlands Institute for Radio Astronomy (ASTRON),
P.O. Box 2, 7990 AA Dwingeloo, The Netherlands
maaskant@astron.nl

[2] Electromagnetic Communication Laboratories,
Pennsylvania State University, University Park, PA 16802, USA
mittra@engr.psu.edu

[3] Faculty of Electrical Engineering, Eindhoven University of Technology,
P.O. Box 513, 5600 MB Eindhoven, The Netherlands
a.g.tijhuis@tue.nl

***Abstract*—** We present a numerically efficient technique, called the Characteristic Basis Function Method (CBFM), for computing the scan impedances of antenna elements located inside an electrically large subarray, which is surrounded by (many) other actively phase-steered subarrays. We construct a reduced moment matrix for a single subarray, and modify its entries in a manner that accounts for the mutual coupling between the surrounding subarrays. This enables us to circumvent the difficult problem of having to deal with the entire large array geometry in one step and reduces the total solve time significantly. Furthermore, the reduced moment matrix can be constructed in a time-efficient manner by exploiting the translation symmetry between pairs of Characteristic Basis Functions (CBFs). However, since we propose an overlapping domain decomposition technique for arrays of electrically interconnected antenna elements, symmetry can only be exploited if the mesh partitioning facilitates a one-to-one mapping of CBFs. To fully utilize the translation symmetry, a strategy has been developed to mesh the structure and to take advantage of this geometrical property. A numerical example is presented for a large array of subarrays of Tapered Slot Antennas (TSAs). The proposed method has good accuracy, excellent numerical efficiency, and reduced memory storage requirement.

***Index Terms*—** Characteristic Basis Function Method, Moment Methods, Scan Impedance, Tapered Slot Antennas, Square Kilometre Array.

I. INTRODUCTION

The Square Kilometer Array (SKA) project is a world-wide project to design and construct a revolutionary new radio telescope with a collecting area which is on the order of 1 million square meters in the wavelength range from 3 m to 1 cm [1–3]. It will have receiver sensitivity orders of magnitude higher than the current radio telescopes in operation, and an unprecedented large instantaneous field-of-view (FOV). The Netherlands institute for radio astronomy (ASTRON) is engaged in the development of the aperture array concept, by designing and examining small-scale prototype arrays, thereby demonstrating the feasibility of the instrument [4]. Concurrently, the knowledge gained from the SKA design studies is being used to realize cost-effective solutions for inexpensive fabrication of the instrument [5]. An electromagnetic field simulation is required at each step to analyze the

1054-4887 © 2009 ACES

antenna impedance and radiation characteristics, which, in turn, facilitates the evaluation of the potentials of various array technologies [6, 7].

In some of these studies it is vitally important to accurately analyze electrically large – but finite – array antenna problems and associated truncation effects. Given the electrical size and geometrical complexity of such structures, the numerical analysis presents a severe computational burden when only limited computing resources are available [8]. In order to mitigate the computational burden, a vast number of numerically efficient techniques have been developed over the last few decades.

In the present paper, we only provide a brief overview of the literature relevant to the approach employed in this paper, namely, iteration-free integral-equation techniques. Moreover, while focusing in this paper on the challenging case of large arrays of strongly coupled TSAs, we point out that the radiation and scattering characteristics of such arrays have been considered by others as well. Much work has been performed on the edge truncation effects and the efficient computation of embedded element patterns and element impedances by the authors of [9], both in the time and the frequency domain. Furthermore, in [10], the Finite Element Method has been combined with an Integral-Equation technique (FEM-IE) to iteratively solve for the fields in TSA arrays that involve dielectric materials.

In this paper, we present an integral-equation-based technique, called CBFM, which enhances the conventional method of moments by compressing the moment matrix such that the resultant reduced matrix equation can be solved in an iterative-free manner, and simultaneously for multiple right-hand sides (MRHS) [11, 12]. The above compression is achieved by employing macro basis functions, which themselves are constructed as fixed combinations (aggregations) of subsectional basis functions [13, 14]. Hence; these macro domain functions can conform to arbitrarily shaped geometries, provided that the underlying subsectional basis functions also satisfy this geometrical property. An additional advantage in using these macro domain functions is that existing computer codes that employ subsectional basis functions can be reused with only minor modifications. Furthermore, in CBFM, the entire computational domain is subdivided into smaller subdomains, each of them supporting a set of numerically generated macro basis functions, referred to herein as CBFs. The inherent advantage of such a domain decomposition technique is that many algorithmic steps involved can be carried out in parallel, on supercomputers or on platforms with multiple processors [15]. Furthermore, the modular setting of a domain decomposition technique enables one to analyze/optimize the entire structure at minimal cost by only reconsidering the domains that have been altered [16].

The concept of reducing the matrix equation by employing numerically generated macro basis functions, and decomposing the problem into smaller problems, has also been widely exploited in other recently developed iterative-free methods for solving large-scale problems. For instance, the Synthetic-Functions Approach (SFX) [17, 18], the Sub-Entire-Domain Basis Function Method (SED) [19], the eigencurrent approach [20], and a subdomain multilevel approach [21]. Although the above methods all have similar objectives, namely to reduce the matrix equation and to solve it in an iterative-free manner, the differences between these methods can be considerable. For example, within the framework of each of these methods, a variety of techniques have been proposed to numerically generate the macro basis functions. Among these, it is possible to distinguish between two categories, namely the overlapping and non-overlapping domain decomposition techniques. Furthermore, different methods have been proposed to ensure that the surface current at the interfaces between adjacent domains are smoothly varying functions without the presence of truncation effects [17, 22]. Obviously, the accuracies of the aforementioned iterative-free methods depend upon the type of domain decomposition employed. In each of these methods, several techniques have been proposed to arrive at a computationally efficient implementation.

For electrically large problems, the overall solution time of CBFM is governed by the time it takes to construct the reduced matrix equation, as opposed to solving it. The construction of the reduced matrix involves the calculation of reaction integrals between pairs of CBFs, for many of which the computation time can be reduced significantly, especially for those that are well-

separated. Various acceleration techniques have been proposed to reduce the matrix construction time, including; multipole approaches [23, 24]; the Adaptive Cross Approximation (ACA) technique [25]; a multi-level decomposition approach [26]; and the Adaptive Integration Method (AIM) [27]. These methods all rely on the fact that the electric field, generated by a macro basis function, is a relatively smoothly varying function over the support of the macro test function. Obviously, the electric field function becomes increasingly smoother over the support of the macro test function, for increasingly large separation distances. Hence, for electrically large antenna and scattering problems, many of the reduced matrix entries (CBF reactions) can be computed rapidly.

In addition to these acceleration techniques, the reciprocity theorem is often used to compute only the upper triangular part of the reduced matrix, and this saves approximately a factor of two in the total fill time. More importantly, and also for array antennas with electrically interconnected antenna elements, a significant degree of translation symmetry exists when the elements are positioned on a uniform grid. This can be understood by realizing that many reactions between (groups of) CBFs are replicated elsewhere in the array. Thus, even though the moment matrix may not have a full block Toeplitz symmetry, many entries (even blocks) of the reduced matrix are identical and, hence, can simply be copied during the matrix construction process. Depending upon the array geometry, the computational complexity of the matrix filling may even be of linear order.

The structure of this paper is as follows. First, we provide a brief description of the CBFM and the steps that are involved in the process of generating a reduced matrix equation, as well as the CBFs for antenna-type problems. Second, we focus on an overlapping domain decomposition technique and describe a strategy for meshing a large array structure efficiently to optimally exploit the translation symmetry between the CBFs. Third, in accordance with the SKA concept of using disjoint phased-array tiles, we outline an approximate technique for an efficient solution for the computation of the scan impedance of antenna elements, located within an electrically large subarray and surrounded by (many) other actively phase-steered subarrays. Results will be presented for a 576 TSA element array, which is subject to several different scanning scenarios, showing that the proposed approximate method is first-order accurate for these types of problems and therefore represents a viable alternative to a full CBFM solution. The significant savings realized in memory and computation time will be described.

II. OUTLINE OF CBFM

A. Domain Decomposition and Matrix Equation Reduction

Let S denote the perfectly conducting surface of an antenna array. In CBFM, we subdivide the entire domain S into N smaller subdomains. N is typically chosen to be equal to the number of antenna elements. If the nth subdomain is denoted by S_n, then

$$S = \bigcup_{n=1}^{N} S_n \,. \tag{1}$$

Since we propose an overlapping domain decomposition technique, $S_p \bigcap S_q \neq 0$, in general, for $p, q \in \{1,2,\ldots,N\}$. However, in our approach, we require that S_p and S_q overlap only if the corresponding antenna elements p and q are electrically interconnected. Furthermore, the overlap is restricted to the adjacent antenna element only. Each subdomain S_n is geometrically represented by an adequate number of triangular patches that are subsequently grouped into pairs to form the Rao-Wilton-Glisson (RWG) vector basis functions used to represent the surface current distribution [28]. Note that as subdomains overlap, some triangular patches, as well as the corresponding RWG basis functions, are common to multiple subdomains. Let N_n denote the number of RWG basis functions on the nth subdomain S_n. Typically, N_n is chosen to be at least 10 RWGs/wavelength in order to achieve a high phase accuracy of the final surface current solution. Moreover, N_n may be governed by tiny geometrical details that need to be represented with sufficient accuracy. Also, let the n^{th} subdomain S_n support a set of K_n CBFs, each of which is expanded using the N_n RWG basis functions. The generation of these CBFs is discussed in Sec. II B. Furthermore, let $\mathbf{J}_n$ be a column-augmented matrix, whose k_n^{th} column vector represents the RWG expansion coefficients of the k_n^{th} CBF on the n^{th} subdomain. Then, if the uncompressed matrix block $\mathbf{Z}_{pq}^{RWG}$ represents the

mutual reaction matrix between the source and test RWGs belonging to domains q and p, respectively, the reduced matrix block $\mathbf{Z}_{pq}^{CBF}$ is readily computed as

$$\mathbf{Z}_{pq}^{CBF} = \left\langle \mathbf{J}_p^T, \mathbf{Z}_{pq}^{RWG} \mathbf{J}_q \right\rangle, \quad (2)$$

where T denotes the transposition operator, and $\langle \cdot,\cdot \rangle$ denotes a symmetric product. Note that the size of the reduced matrix block $\mathbf{Z}_{pq}^{CBF}$ is $K_p \times K_q$, whereas the uncompressed matrix block $\mathbf{Z}_{pq}^{RWG}$ is of size $N_p \times N_q$.

Similarly, if the uncompressed RWG excitation vector for the pth subdomain is denoted by $\mathbf{V}_p^{RWG}$, and its size is $N_p \times 1$ (single excitation), the reduced excitation vector $\mathbf{V}_p^{CBF}$ is of size $K_p \times 1$, and is computed by evaluating

$$\mathbf{V}_p^{CBF} = \left\langle \mathbf{J}_p^T, \mathbf{V}_p^{RWG} \right\rangle. \quad (3)$$

Finally, after constructing all the reduced matrix blocks, as well as the reduced excitation vectors for all subdomains, we obtain a reduced matrix equation that has the form

$$\mathbf{Z}^{CBF} \mathbf{I}^{CBF} = \mathbf{V}^{CBF}, \quad (4)$$

which can be solved directly for the unknown CBF expansion coefficient vector $\mathbf{I}^{CBF}$, in an iteration-free manner, provided that the size of $\mathbf{Z}^{CBF}$ is sufficiently small. In fact, depending upon the type of problem and required solution accuracy, the size of vector $\mathbf{I}^{CBF}$ can be a factor 50-500 smaller than $\mathbf{I}^{RWG}$.

B. Generation and Windowing of CBFs

A rather attractive feature of the physics-based CBFM is the way CBFs are generated. We will briefly describe this procedure for an overlapping domain decomposition approach, applied to antenna array problems. The details can be found in several previously published works [12, 22] and [25].

For large antenna array problems, we first extract several distinct and relatively small subarrays from the fully meshed array, typically from the center, corners and edges of the array. The subarray sizes are chosen such that the direct electromagnetic environment for the center, corner and edge elements of the corresponding subarrays closely resemble their original electromagnetic array environment. For instance, Fig. 1b illustrates two subarrays that are extracted from a $4 \times 3 \times 2$ dual-polarized Vivaldi array[1]. These two subarrays represent a corner and center element along with their interconnected neighboring elements, respectively.

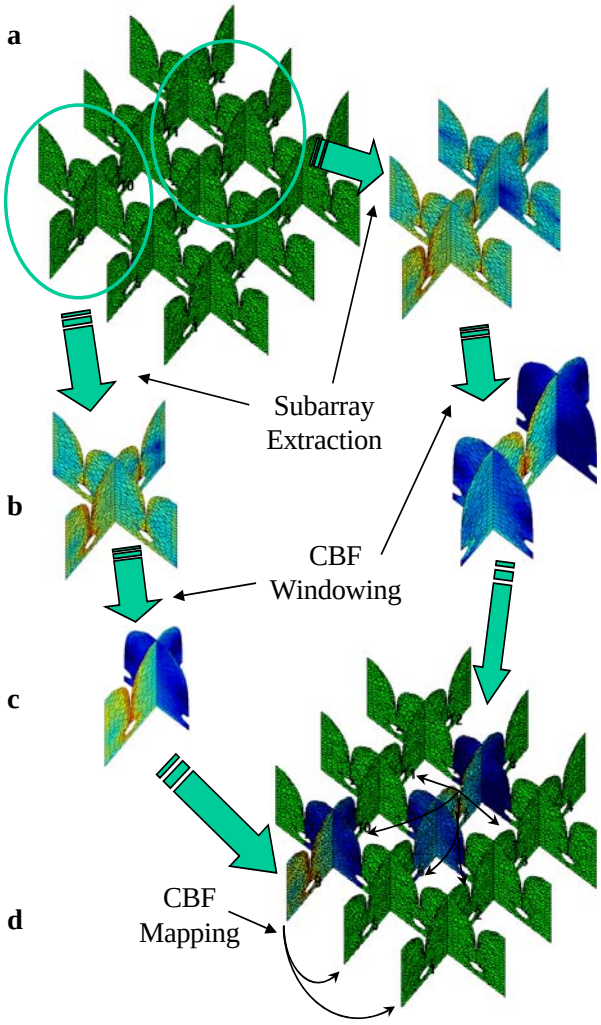

Fig. 1. Approach to generate and window primary CBFs. (i) Subarray extraction and generation of primary CBFs, (ii) Trapezoidal post-windowing of CBFs, (iii) One-to-one mapping of CBFs throughout the array lattice.

Next, we solve for a set of surface currents induced in each of the subarrays, by sequentially exciting the antenna terminals of the corresponding subarray (Fig. 1b). Hence, for our example, 4 primary CBFs are generated for the subarray comprising the corner element, and 7 primary CBFs for the subarray comprising the center element.

[1] 4 elements in the E-plane, 3 elements in the H-plane, and 2 polarizations.

Next, we apply a (trapezoidal) post-windowing function to the sets of primary CBFs to suppress the undesired edge-truncation effects by reducing the support of the so-generated primary CBFs (Fig. 1c). In essence, the RWG expansion coefficients making up the CBFs are post-multiplied with suitable weights. Note that the partially overlapping windowing functions have to add up to unity, so that the tapered CBFs add up in a correct manner as well, particularly in the overlapping regions. In our specific example (Fig. 1), the support extends to one-half of the neighboring elements, though this can be changed in a manner discussed in [22]. For instance, in [25], very good accuracy has been realized with only a one-cell overlap.

Finally, the set of CBFs are mapped, one-to-one, onto the corresponding edge and center elements so that each array-element/subdomain will have its own set of CBFs (Fig. 1d). Note that for our example, 6 subarrays have to be extracted in total so as to accommodate CBFs on all the array elements (3 subarrays per polarization, i.e., 2 subarrays for the opposite edge elements, and 1 for a center element).

The number of CBFs on array elements can be enlarged in order to model surface currents on array elements that can have a large degree of freedom, namely, by appending a set of secondarily generated CBFs to the already existing set of primary CBFs [12]. This is accomplished by taking the primary CBFs as distant current sources to the subarrays, which then induce extra surface currents on these subarrays after which these newly generated currents are truncated/windowed again and added to the primary set of CBFs.

Regarding the generation of CBFs, it is instructive to consider how the CBFs differ from eigencurrents employed in the eigencurrent approach [20]. In CBFM, the induced surface current on each subarray is computed for a certain excitation vector $\mathbf{V}$ by solving the corresponding matrix equation $\mathbf{ZI} = \mathbf{V}$ for the unknown RWG expansion coefficient vector $\mathbf{I}$. The complex symmetric moment matrix $\mathbf{Z} = \mathbf{Z}^T$ is assumed to be nondefective and diagonalizable by its eigenvectors. Hence, an eigenvalue decomposition of $\mathbf{Z}$ exists and is herein expressed through the block factorization

$$\mathbf{Z} = \mathbf{UDU}^{-1}, \tag{4}$$

where the n^{th} diagonal entry ν_n of diagonal matrix $\mathbf{D}$ is the nth eigenvalue of $\mathbf{Z}$, and where the nth column $\mathbf{u}_n$ of $\mathbf{U}$ is the nth eigenvector of $\mathbf{Z}$. Hence, the unknown coefficient vector $\mathbf{I}$ can be expressed in terms of the eigenvectors $\mathbf{u}$, eigenvalues ν, and excitation vector $\mathbf{V}$ as

$$\mathbf{I} = \sum_{n=1}^{N} \frac{1}{\nu_n} \left\langle \mathbf{u}_n, \mathbf{V} \right\rangle \mathbf{u}_n . \tag{5}$$

In the eigencurrent approach [20], the eigencurrents $\mathbf{u}$ of $\mathbf{Z}$ are used as macro-domain basis functions. Essentially, the set of eigencurrents forms a fingerprint of the physical structure and simultaneously forms a complete orthonormal basis for the currents that can exist on this structure. Accurate solutions have been obtained for arrays of disconnected antenna elements, by using only an (incomplete) subset of $\mathbf{u}$. However, this reduced orthonormal basis does not include information about the port position of the antenna element or excitation field applied to the actual problem, and therefore will, in general, not lead to the most optimal/smallest basis. On the contrary, in CBFM, a representative excitation field $\mathbf{V}$ is applied to each subarray to generate CBFs, implying that we identify the left-hand-side of (5) as a basis. This can be advantageous, because when an antenna port of a subarray is excited, the induced surface current (and thus the CBF) naturally accounts for a possibly asymmetrical port position, and may therefore represent the final surface current quite well even when we employ only a limited number of the above macro-domain basis functions. However, one major drawback in generating macro basis functions in this manner is that these CBFs will not be mutually orthogonal in general. As a remedy, one would need to orthonormalize the CBFs, and retain only a minimal number of them. This can both be accomplished with the aid of a Singular Value Decomposition (SVD) and a thresholding procedure on its singular values [29, 30].

III. EXPLOITING TRANSLATION SYMMETRY

Once each (extended) subdomain supports a set of CBFs, the reduced moment matrix can be constructed efficiently by exploiting the translation symmetry. As an example, Fig. 2

graphically exemplifies that the reduced matrix block $\mathbf{Z}_{pq}^{CBF}$ equals $\mathbf{Z}_{p+1;q+1}^{CBF}$, because both blocks represent reactions between identical, though translated, set of CBFs.

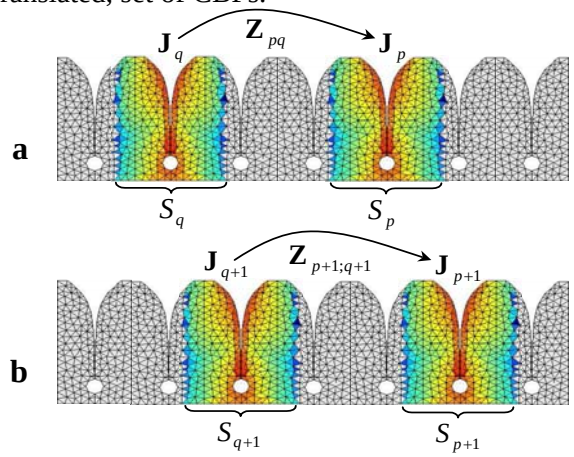

Fig. 2. Construction of identical reduced matrix blocks $\mathbf{Z}_{pq}^{CBF}$ and $\mathbf{Z}_{p+1;q+1}^{CBF}$.

Therefore,

$$\mathbf{Z}_{pq}^{CBF} = \left\langle \mathbf{J}_p^T, \mathbf{Z}_{pq}^{RWG} \mathbf{J}_q \right\rangle = \mathbf{Z}_{p+1;q+1}^{CBF}, \qquad (6)$$

provided that the extended subdomain S_q (Fig. 2a), that supports a set of source CBFs, maps one-to-one onto the one-element translated subdomain S_{q+1} (Fig. 2b). Furthermore, the testing CBFs supported by the subdomain S_p have to map one-to-one onto the subdomain S_{p+1} when the same translation vector is used. However, this requires a consistent triangulation as well as a consistent partitioning of the RWGs of all subdomains (and thus array elements) as further clarified with the aid of Fig. 3.

A. Array Meshing Method

The entire array mesh can be efficiently constructed from a few elementary meshed array elements, called the base elements. The geometry of each base element is discretized by a number of polygonal facets of which the outlines are described by a set of boundary nodes. Figure 3 (Step I) shows a discretized TSA base element comprising of 3 polygonal surfaces (two tapered fins and one tiny port polygon across the slotline), where the polygonal boundary nodes are designated by (red) dots. Every polygonal facet is supplied by a non-uniform grid of internal nodes and subsequently triangulated (in a 2-D plane) using a Delaunay meshing routine [31, 32]. The internal grid is distributed such that the elementary triangles are very nearly equilateral. Subsequently, nodes and triangles are added along the boundaries to ensure that the triangulations will be consistent with those of the electrically interconnected adjacent elements when these base elements are placed in the array environment. Next, triangulated base elements are equipped with the RWGs. Step I (Fig. 3) shows a possible RWG polarity distribution, visualized by vectors that join the common edges of each pair of triangles to form an RWG.

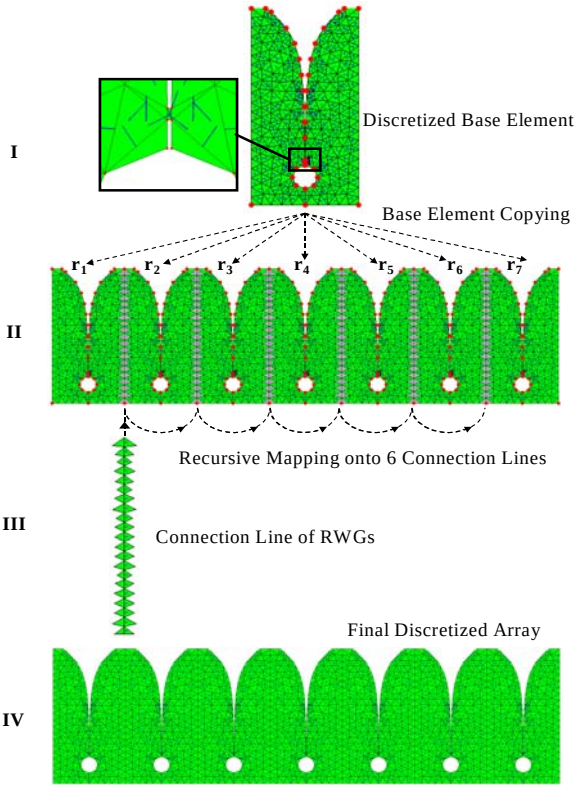

Fig. 3. Efficient and consistent meshing of the antenna array structure to fully exploit translation symmetry.

Step II illustrates a one-to-one replication of the discretized base element at array element locations $\boldsymbol{r}_1 \ldots \boldsymbol{r}_7$. Note that, at this stage, the RWGs ensuring the electrical connection between array elements have not yet been defined. This is accomplished in Step III, where the triangles along a connection line are separately equipped with RWGs and subsequently mapped (recursively) onto the various corresponding connection lines that remain to be equipped with RWGs. For this purpose, we utilize the array symmetry as detailed in the next section. A pseudo code of the

recursive-mapping algorithm is included in App. A using Matlab's notation.

Finally, a full meshing of the array geometry (Step IV) facilitates a one-to-one mapping of the CBFs, even though each supporting subdomain extends beyond the outer boundaries of an array element, as shown in Fig. 2.

B. Array Symmetry Extraction Method

For the full array geometry, the degree of translation symmetry between pairs of subdomains, each of which supports a set of CBFs, can be determined as explained below. Following the generation of the boundary nodes for the array in a manner shown in Fig. 3 of Step-II where we replicate the boundary nodes of the base element(s) at their respective array positions, we can determine which array elements are electrically interconnected. Furthermore, when using multiple base elements, such as in the case of dual-polarized arrays, one can also keep track of the type of base element that is interconnected. Let the element interconnection and the corresponding base element type be stored in two separate matrices. Then, for our example, using only one type of base element (Fig. 3), we have:

$$\begin{bmatrix} 1 & 2 & 0 \\ 2 & 1 & 3 \\ 3 & 2 & 4 \\ 4 & 3 & 5 \\ 5 & 4 & 6 \\ 6 & 5 & 7 \\ 7 & 6 & 0 \end{bmatrix} \quad \text{and} \quad \begin{bmatrix} 1 & 1 & 0 \\ 1 & 1 & 1 \\ 1 & 1 & 1 \\ 1 & 1 & 1 \\ 1 & 1 & 1 \\ 1 & 1 & 1 \\ 1 & 1 & 0 \end{bmatrix}$$

where the first rows of the left- and right-hand matrices indicate that element-1 is connected to element-2, and that they are both base elements of type-1 (ignore the zero entries).

Also, for each array element, one can determine the relative positions of the electrically interconnected elements surrounding it. Upon comparing the groups of relative position vectors in conjunction with the corresponding base element types (rows of second matrix), one can readily determine which subdomains (and therefore corresponding set of CBFs) are identical. For our example, subdomains {2, 3, 4, 5, 6}; {1}; and {7} form 3 unique groups. As explained in Section II B, we need to only generate one set of CBFs per unique subdomain, in this case for subdomains 1, 7 and 4, where subdomain 4 is chosen from the first group as the most centralized element. Elements 1, 7 and 4 are extracted from the fully meshed array, together with their neighboring array elements (within a specified radius), to form the resulting three subarrays that are used to generate the CBFs. Note that, after windowing these CBFs, the CBFs supported by subdomain 4 are mapped onto the subdomains 2, 3, 5 and 6.

After determining the unique subdomains (1, 4 and 7), from which the CBFs are mapped, we also compute the relative element array position vectors between all the array elements and store these in a matrix form. For our example, we have

$$\begin{bmatrix} \mathbf{r}_1 - \mathbf{r}_1 & 1 & 1 \\ \mathbf{r}_1 - \mathbf{r}_2 & 1 & 4 \\ \mathbf{r}_1 - \mathbf{r}_3 & 1 & 4 \\ \vdots & \vdots & \vdots \\ \mathbf{r}_7 - \mathbf{r}_5 & 7 & 4 \\ \mathbf{r}_7 - \mathbf{r}_6 & 7 & 4 \\ \mathbf{r}_7 - \mathbf{r}_7 & 7 & 7 \end{bmatrix},$$

where the first column holds the 49 relative array position vectors between element pairs, and the last two columns denote the corresponding two array elements that support the same set of CBFs from which they were initially mapped, namely either 1, 4 or 7. By comparing the rows, one can readily determine which element/subdomain pairs are identical in terms of the sets of CBFs supported by them (last two columns), as well as their mutual orientation and separation distance (first column). Upon selecting the unique rows, the minimal number of impedance matrix blocks that need to be filled can be determined (out of the 49 possible combinations). For convenience, we create a new matrix showing how the reduced matrix is built-up from only a limited number of unique matrix blocks. For our example, the structure of the 7x7 block matrix is:

Subdomain #	***1***	***2***	***3***	***4***	***5***	***6***	***7***
1	1	2	3	4	5	6	7
2		8	9	10	11	12	13
3			8	9	10	11	14
4				8	9	10	15
5					8	9	16
6						8	17
7							18

where only 18 out of 49 non-redundant mutual impedance blocks have been identified, since we also exploited reciprocity (only the upper triangular part of the matrix is required). Note that, for this example, the matrix entry 11 denotes that the reactions between the CBFs supported by subdomains 2 and 5 are identical to the reactions between the CBFs supported by subdomains 3 and 6, as we can verify by using Fig. 3.

In summary, symmetry can be exploited for arrays of electrically interconnected elements to reduce the complexity of the matrix filling process. For the present example (Fig. 3), the computational complexity becomes linear when the symmetry is exploited.

Furthermore, symmetry can also be used to efficiently compute the array far-field pattern function $\mathbf{f}^{tot}$ by expanding $\mathbf{f}^{tot}$ in terms of M known CBF far-field patterns $\mathbf{f}^{CBF}$ as follows (see also [23]):

$$\mathbf{f}^{tot}(\theta,\varphi) = \sum_{m=1}^{M} I_m^{CBF} \mathbf{f}_m^{CBF}(\theta,\varphi), \qquad (7)$$

where I_m^{CBF} is the mth expansion coefficient for the mth CBF. The coefficient vector $\mathbf{I}^{CBF}$ is computed via the CBFM for a certain array excitation. Because many of the subdomains support the same set of CBFs, the respective CBF patterns are identical as well, apart from a phase correction due to their translated position. For instance, we can write

$$\mathbf{f}_p^{CBF} = \mathbf{f}_q^{CBF} e^{-jk\langle \mathbf{r}_{pq}, \hat{\mathbf{r}}(\theta,\varphi)\rangle}, \qquad (8)$$

where the p^{th} CBF pattern is derived from the qth one by accounting for the translation vector $\mathbf{r}_{pq}$. The unit vector $\hat{\mathbf{r}}(\theta,\varphi)$ denotes the direction of observation, and k the free-space wavenumber of the medium. Note that, for our example (Fig. 3), we only need to explicitly compute the CBF patterns for the sets of CBFs supported only by the subdomains 1, 4 and 7. The remaining CBF patterns are obtained simply via translation.

IV. ARRAYS OF ELECTRICALLY LARGE SUBARRAYS

A rigorous full-wave analysis of phased arrays, each of them surrounded by a number of other disjoint actively phased-steered arrays, becomes computationally prohibitive for a large number of electrically large subarrays. Despite the fact that the computational complexity of solving the matrix equation can be reduced by a large factor by employing a relatively small number of CBFs, the numerical analysis of a much larger array of subarrays will inevitably pose a computational burden, along with an increase in the number of unknowns beyond a certain point. Conventional infinite array approaches may be accurate and fast for an extremely large array of subarrays, although the subarrays have to be electrically small and positioned over a uniform (possibly skewed) rectangular lattice.

In the method proposed herein, the CBFM is used to construct a reduced moment matrix for only one of the subarrays, and the matrix entries are modified so as to account for the mutual coupling by using the characterization of the actively phase-steered surrounding subarrays. Towards this end, we enforce the final surface current solution to be identical on every subarray, apart from a phase difference depending on the scan angle and position vector of a subarray, whereas within each subarray, surface currents may differ per element.

Computing the fields in a given region of a periodic structure, while assuming that they are identical in other regions is a perturbation approach, has also been exploited by Skrivervik and Mosig [33, 34]. The first exposes a spectral-domain approach, the latter shows a spatial-domain approach. In its implementation, the latter is closer to the approach considered in this paper; the main difference being that in the Skrivervik and Mosig papers, the region referred to above is one (microstrip) antenna, while in this paper, it corresponds to a sub-array.

Basically, the CBFM is used at antenna element level, whereas an infinite array approach is used at subarray level. The concept of combining infinite array approaches with macro-domain basis-functions have been examined before in similar methods, e.g., in [35] and [36].

The use of an infinite array assumption at the subarray level obviates the need to solve for all the subarrays at once, and reduces the total solve-time significantly. Obviously, such an approximate method is exact for infinite arrays of mutually coupled subarrays, as well as for finite arrays of non-coupled subarrays (isolated subarrays), or for mutually coupled subarrays where the end-effects of bordering subarrays do not disrupt the

impedance characteristics of the subarray under study. Hence, for a finite and all-excited array, the active mutual coupling (or active mutual scan impedance) between the subarrays is one of the primary factors that determines the approximation error of the proposed method. Generally, the accuracy of the approximate method depends upon the scan angle, number of surrounding subarrays, the electrical distance between the subarrays, the electrical size of a subarray, and the type of the antenna element.

Let us refer to Fig. 4, in which we depict the scheme for computing the scan impedance matrix of the six antenna elements that comprise the central subarray. Basically, the scan impedance matrix is obtained by adding the phase-shifted coupling impedance matrices of the surrounding subarrays to the array impedance matrix of the central subarray.

As we impose the condition that the final surface current solutions among the various subarrays be identical, except for a phase shift, we are led to conclude that the corresponding CBF expansion coefficients have to be equal, though phase shifted as well. Figure 4a illustrates how the (active) reduced matrix block $\mathbf{Z}_{pq}^{CBF}$ is computed by testing the electric field, which is generated not only by the source CBF $\mathbf{J}_q$, but also by the respective phase-shifted neighboring source CBFs $\mathbf{J}_q e^{j\phi}$ and $\mathbf{J}_q e^{-j\phi}$ (coupling terms), where the phase shift ϕ depends on both the scan direction $\hat{\mathbf{r}}(\theta,\varphi)$ and the relative position of the subarray w.r.t. the central subarray.

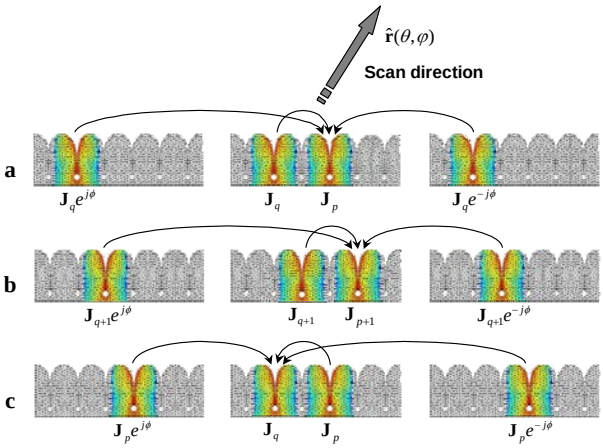

Fig. 4. Reduced matrix construction for the central subarray while accounting for the coupling with the actively phase-steered surrounding subarrays.

In the process of computing all the mutual reactions, the translation symmetry can again be exploited for fast construction of the $\mathbf{Z}^{CBF}$. This can be observed by comparing Fig. 4a to Fig. 4b (see also Sec. III), where an identical though one-element translated reaction between the CBFs is visualized.

Finally, for an off-broadside scan direction, one can easily verify that the active reduced matrix block $\mathbf{Z}_{pq}^{CBF} \neq \left(\mathbf{Z}_{qp}^{CBF}\right)^T$. This is depicted in Fig. 4c, where the source and test domains on the central subarray have been interchanged with respect to the domains shown in Fig. 4b. Consequently, the final active reduced matrix $\mathbf{Z}^{CBF}$ will be non-symmetric; therefore, both the upper- and lower-triangular part of the matrix must be computed, at least partially.

V. NUMERICAL RESULTS

The numerical accuracy and efficiency of the modified CBFM approach, relative to a direct CBFM approach, will be evaluated in this section for an array of disjoint subarrays of TSA elements. The anomalous antenna impedance effects, associated with the (resonant) gaps/slots between disjoint subarray tiles, have been reported in [37, 38] and will therefore not be discussed in this paper. These gaps may need to be introduced for servicing purposes, so that, e.g., individual subarrays can be installed and/or removed as modular units. Furthermore, the transport and manufacturability of relatively small units may be advantageous.

Unless specified otherwise, a threshold of 10^{-2} is used both for the SVD procedure in CBFM, and in the Adaptive Cross Approximation Algorithm [25]. These parameter settings are chosen to be equal for both the direct and modified CBFM approach and we will exploit the translation symmetry for all the cases that are studied, which enables us to make relative comparisons.

All the computations have been carried out by using double-precision arithmetic on a Dell Inspiron 9300 Notebook, equipped with an Intel Pentium-M processor operating at 1.73 GHz, and 2.0 GB of RAM.

The TSA element geometry has been adopted from [22] and [25], and serves here as a reference case for further study.

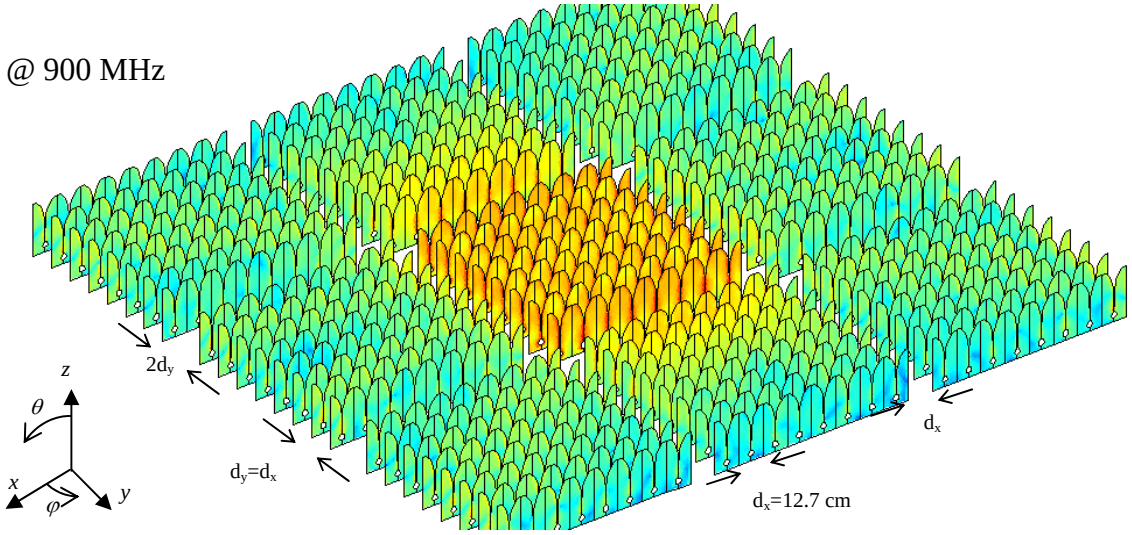

Fig. 5. Array of 9 subarrays (3x3), each of them composed of 64 TSA elements (8x8). To illustrate coupling effects, the active antennas within the central tile are excited by a voltage-gap generator placed over the slot of each TSA element. The central tile scans to broadside (end-fire direction), whereas the TSAs of the surrounding tiles are short-circuited. The magnitude of the surface current distribution is shown (log scale) as computed by a direct CBFM approach.

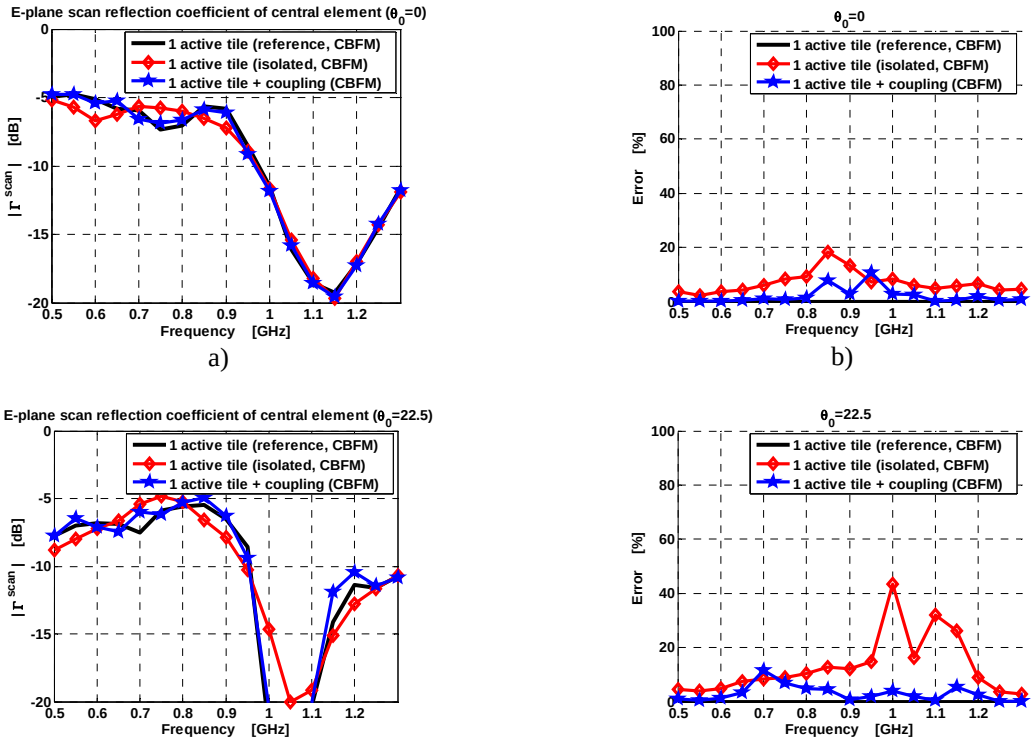

Fig. 6. (a) Scan reflection coefficient of the central element of the central subarray for broadside scan; (b) Average relative error of all the scan reflection coefficients of the central tile\subarray, for broadside scan; (c) Scan reflection coefficient of the central element of the central subarray for a 22.5 Deg E-plane scan; (d) Average relative error of all the scan reflection coefficients of the central tile\subarray, for a 22.5 Deg E-plane scan.

@ 900 MHz (θ_0=0)	# RWGs	# CBFs	# MoM Blocks	# MoM Blocks (Symmetry)	Time to build MoM blocks	Total Execution Time
9 Tiles	375192	4320	331776	8394	144 m. 29 s.	209 m. 25 s.
1 Isolated Tile	41688	464	4096	294	3 m. 54 s.	11 m. 45 s.
1 Tile + Coupling	41688	480	4096	294	8 m. 42 s.	16 m. 48 s.

Figure 5 illustrates an array of 9 TSA subarrays (3×3) for which a total of 375,192 RWG basis functions have been employed. We compute the antenna impedance matrix of the 576 TSA elements by using a direct CBFM approach, and then go on to derive the scan reflection coefficient for each TSA element (150Ω source-reference impedance). These scan reflection coefficients are taken as references for further comparison. It should be noted that the scan impedances (or scan reflection coefficients) are not only of interest for the characterization of transmit antennas, but can also be used to evaluate noise coupling in receive antennas [39, 40].

Let the scan reflection coefficient of the *n*th antenna element be denoted as Γ_n^{scan}, and the total number of the central subarray elements be N_{sub}. Then, within the central subarray, the average relative error between the actual and approximated scan reflection coefficients can be defined as

$$Error = \frac{\sum_{n}^{N_{sub}} |\Gamma_n^{scan,ref}(\theta_0,\varphi_0) - \Gamma_n^{scan,approx}(\theta_0,\varphi_0)|^2}{\sum_{n}^{N_{sub}} |\Gamma_n^{scan,ref}(\theta_0,\varphi_0)|^2} \times 100\% \quad (9)$$

where θ_0 and φ_0 designates the scan direction. For the sake of comparison, the error in the scan reflection coefficients has been computed for a single isolated subarray, as well as for a single subarray where we account for the coupling effects with the neighboring subarrays (Sec. IV). Figures 6a and 6c show the scan reflection coefficient of the central element of the central subarray, obtained by using the direct CBFM (reference solution). The same figures also plot the results obtained by using both the single isolated subarray configuration and the subarray configuration with coupling. The corresponding average relative errors for the two scan directions have been plotted in Figs. 6b and 6d as a function of the frequency for the reference case; the isolated array case; and, for the approximate method as proposed in this paper.

As compared to the single isolated subarray case, the accuracy of the scan reflection coefficients is higher for the one-tile array with coupling, particularly for off-broadside scan directions. Obviously, a relatively good accuracy can be obtained for a solve time that is comparable to the time required to solve a single isolated subarray problem (~17 min. versus ~12 min.). The larger solve time is due to the overhead required to construct the reduced matrix while accounting for the coupling terms with neighboring subarrays. Despite this overhead, the overall solve time is about 12 times shorter than the total time required when we use the CBFM approach.

VI. CONCLUSIONS AND FUTURE WORK

In this paper we have outlined a strategy for meshing arrays of electrically interconnected antenna elements in a manner that optimally exploits the translation symmetry between the groups of Characteristic Basis/Testing Functions. As a consequence, the reduced matrix has a block Toeplitz structure and can therefore be constructed in a numerically efficient manner by realizing that many matrix blocks are identical and, hence, can be simply copied during the matrix generation process. The complexity of the matrix-filling process can be reduced to linear order, for 1-D arrays of interconnected single-polarized antennas, by exploiting the Toeplitz symmetry.

In addition, an approximate method has been presented for computing the antenna scan impedances of elements within a subarray, which is surrounded by (many) disjoint phased-steered subarrays. The reduced matrix is constructed only for one of the subarrays, while the coupling between the adjacent subarrays is accounted for explicit in the process of constructing the reduced matrix. Numerical results have been shown for the central subarray of an array of 9 subarrays of 64 tapered slot antennas each. It was shown that the scan reflection coefficients of a single isolated tile resemble those of a central tile which is surrounded by 8 phase-steered subarrays. However; a higher accuracy was obtained for the proposed approximate technique, where a single subarray has been considered while accounting for the coupling with the neighboring subarrays. As expected, the accuracy remains reasonably good (error is less than 10%) for off-broadside scan directions. The total solve time is approximately 12 times faster than that of the direct CBFM approach, though the result has to be recomputed for each scan angle. It should be noted that the scan impedances (or scan reflection coefficients) are not only of interest for the characterization of transmit antennas, but can also be used in the

evaluation of noise coupling in receive antennas [39, 40].

In this paper we enforce the condition that the final surface current solution be identical on each subarray, apart from a phase difference depending upon the scan angle and position vector of a subarray, though the surface currents may differ per element within each subarray. It is conjectured that the solution accuracy can be further increased by post-correcting the amplitude level of the initially computed solution of the current per subarray, while maintaining their shapes. For our example, we then have to solve a system of 9 unknowns (per scan angle) in order to accurately synthesize the edge effects in current amplitudes of bordering subarrays.

APPENDIX

The mapping of the 6 consecutive connection lines of RWGs (Fig. 3, step III) is straightforward when we use the array symmetry as described in Sec. III B. For this procedure, a recursive mapping algorithm is employed, which has been developed and summarized below using a pseudo Matlab notation.

Essentially, the main program is executed to construct a list of connection RWGs, termed *ConnRWGList*, which holds the final set of connection RWGs for all lines. To build this list, we first iterate over all RWG connection lines that have been identified (6 identical lines in Fig. 3, although, in general, many more lines may exist that are different from one another). During each iteration, we select a line that is free of RWGs, then equip this line with RWGs, and map this line onto the corresponding translated lines that are yet to be equipped with RWGs, and in a recursive manner by invoking the function *MapRWGLine*.

Main program to build a list of all connection RWGs:

```
ConnRWGList=[];
for n=1:NumberOfConnectionLines
          if triangles along nth line without RWGs?
      -    Equip these connection triangles with
           ConnectionRWGs;
      -    rOffsetGlobal=rOffsetList=[0 0 0];
      -    Call recursive function:
           [ConnectionRWGs, rOffsetList]=MapRWGLine
           (rOffsetGlobal, ConnectionRWGs, rOffsetList,
           ConnRWGList);
      -              Append ConnectionRWGs to
   ConnRWGList;
          end
end
```

The recursive function *MapRWGLine* (detailed on second last page) determines which subdomains are sharing the present RWG connection line at hand. We iterate over the pertaining subdomains and determine, for each subsequent subdomain, which other subdomains are equal, in the sense that they support the same set of CBFs. Within this first loop, we then also iterate over the equal subdomains and, during each iteration, compute the corresponding relative position vector of the corresponding identical subdomain. Within this second loop, we translate/map the RWG line under consideration using the same relative position vector, except if we have mapped this line to the same position before. After the mapping has been successfully completed, we recall the recursive function at this newly mapped position.

The total recursion depth is approximately equal to the total number of maps that have to be made. When the procedure returns from the deepest recursion, most of the maps have been carried out so that the double loops within each recursion are not as time-demanding as one may think at a first glance, because identical maps are skipped. However, the double loop is required to ensure that one also maps the RWG connection line onto the left-hand-side of element 7 (Fig. 3) for instance, which is not obvious by only considering the identical subdomains that belong to subdomain 2.

Recursive function `MapRWGLine`:

```
[ConnRWGList, rOffsetList]=MapRWGLine
(rOffsetGlobal, ConnectionRWGs, rOffsetList, ConnRWGList)
     -    Determine subdomains/elements attached to the
          connection line under consideration;
    for m=1:NumberOfAttachedSubDomains
         - Determine list of subdomains that are
           equal to this mth attached subdomain;
                  for k=1:NumberOfEqualSubDomains
             -   Compute rel. pos. vector rOffset
                 between mth attached subdomain and kth
                 equal subdomain;
             -   rOffsetGlobalNew = rOffsetGlobal +
                                    rOffset;
           if rOffsetGlobalNew not in rOffsetList?
                 -   Append rOffsetGlobalNew to
                     rOffsetList;
                 -   Map ConnectionRWGs using rOffset,
                     yielding MappedRWGs;
                 -   Append MappedRWGs to ConnRWGList;
                 -   Call the recursive function:
                     [ConnRWGList, rOffsetList]=MapRWGLine
                     (rOffsetGlobalNew, MappedRWGs,
                     rOffsetList, ConnRWGList)
           end
        end
    end
```

ACKNOWLEDGEMENT

We are grateful to Prof. A. Boryssenko from Amherst University (UMASS) for his advices and suggestions regarding the implementation of a MATLAB mesher.

REFERENCES

[1] P. J. Hall, "The square kilomtere array: an engineering perspective," Reprinted from *experimental astronomy*, vol. 17, no. 1-3, 2004, ISBN: 1-4020-3797-x, Springer 2005.

[2] A. B. Smolders and M. P. van Haarlem, "Perspectives on radio astronomy: technologies for large antenna arrays," *Conf. Proc., ASTRON*, ISBN: 90-805434-2-x, April 1999.

[3] Website: http://www.skatelescope.org/

[4] A. van Ardenne and C. M. de Vos, "EMBRACE (Electronic Multi-Beam Radio Astronomy ConcEpt) an update 2005," SKA meeting, Pune, India, 2005.

[5] R. Maaskant, M. Popova, and R. van de Brink, "Towards the design of a low cost wideband demonstrator tile for the SKA," *Proc. European Conf. on Antennas and Propag. EUCAP*, Nice, France, 2006.

[6] R. Maaskant, R. Mittra, and W. van Cappellen, "Efficient numerical analysis of prototype antennas for the Square Kilometer Array (SKA) using the Characteristic Basis Function Method (CBFM)," *IEEE AP-S International Symposium USNC/URSI Meeting*, Albuquerque, New Mexico, Jul. 9-14, 2006.

[7] R. Maaskant, M. Ivashina, R. Mittra, W. Yu, and N. T. Huang, "Parallel FDTD modeling of a focal plane array with Vivaldi elements on the highly parallel LOFAR Bluegene/L supercomputer," *IEEE AP-S International Symposium*, Albuquerque, New Mexico, pp. 3861-3864, July 2006.

[8] R. Mittra, "A look at some challenging problems in computational electromagnetics," *IEEE Antennas Propag. Mag.*, vol. 46, no. 5, pp. 18-32, Oct. 2004.

[9] C. Craeye, A. O. Boryssenko, and D. H. Schaubert, "Analysis of infinite and finite arrays of tapered-slot antennas for SKA," *Proc. EUMC*, Milan, Italy, pp. 1003-1006, 2002.

[10] M. N. Vouvakis, S. C. Lee, K. Zhao, and J. F. Lee, "A symmetric FEM-IE formulation with a single-level IE-QR algorithm for solving electromagnetic radiation and scattering problems," *IEEE Trans. Antennas Propag.*, vol. 52, no. 11, pp. 3060-3070, Nov. 2004.

[11] V. Prakash and R. Mittra, "Characteristic basis function method: A new technique for efficient solution of method of moments matrix equations," *Micro. Opt. Tech*. vol. 36, pp. 95-100, Jan. 2003.

[12] J. Yeo, V. Prakash, and R. Mittra, "Efficient analysis of a class of microstrip antennas using the Characteristic Basis Function Method (CBFM)," *Micro. Opt. Tech*. vol. 39, pp. 456-464, Dec. 2003.

[13] G. A. E. Vandenbosch and A. R. Van de Cappelle, "Use of combined expansion scheme to analyze microstrip antennas with the method of moments," *Radio Sci.*, vol. 27, pp. 911-916, Nov. /Dec. 1992.

[14] J. Heinstadt, "New approximation technique for current distribution in microstrip array antennas," *Micro. Opt. Tech*. vol. 29, pp. 1809-1810, Oct. 1993.

[15] E. Lucente and A. Monorchio, "A parallel iteration-free MoM algorithm based on the Characteristic Basis Functions Method," *Proc. int. URSI Commission B, EMTS 2007*, Ottawa, Canada, July 26-28, 2007.

[16] A.M. van de Water, B. P. de Hon, M. C. van Beurden, A. G. Tijhuis, and P. de Maagt, "Linear Embedding via Green's operators: A modeling technique for finite electromagnetic band-gap structures," *Phys. Rev. E*, vol. 72, p. 056704, 2005.

[17] L. Matekovits, V. A. Laza, and G. Vecchi, "Analysis of large complex structures with the synthetic-functions approach," *IEEE Trans. Antennas Propag.*, vol. 55, no. 9, pp. 2509-2521, Sep. 2007.

[18] L. Matekovits, G. Vecchi, G. Dassano, and M. Orefice, "Synthetic function analysis of large printed structures: the solution space sampling approach," *IEEE AP-S International Symposium*, Boston, Massachusetts, pp. 568-571, July 2001.

[19] W. B. Lu, T. J. Cui, Z. G. Qian, X. X. Yin, and W. Hong, "Accurate analysis of large-scale periodic structures using an efficient Sub-Entire-Domain basis function method," *IEEE Trans. Antennas Propag.*, vol. 52, no. 11, pp. 3078-3085, Nov. 2004.

[20] D. J. Bekers, S. J. L. van Eijndhoven, A. A. F. van de Ven, P. Borsboom, and A. G. Tijhuis, "Eigencurrent analysis of resonant behavior in finite antenna arrays," *IEEE*

Trans. Micro. Theory Tech., vol. 54, no. 6, pp. 2821-2829, June 2006.

[21] E. Suter, J. R. Mosig, "A subdomain multilevel approach for the efficient MoM analysis of large planar antennas," *Micro. Opt. Tech.* vol. 26, no. 4, pp. 270-277, Aug. 2000.

[22] R. Maaskant, R. Mittra, and A. G. Tijhuis, "Application of trapezoidal shaped Characteristic Basis Functions to arrays of electrically interconnected antenna elements," *Proc. Electromagnetics in Advanced Applications*, ICEAA, pp. 567-571, 17-21 Sept. 2007.

[23] C. Craeye, "A fast impedance and pattern computation scheme for finite antenna arrays," *IEEE Trans. Antennas Propag*., vol. 54, no. 10, pp. 3030-3034, Oct. 2006.

[24] E. Garcia, C. Delgado, F. S. de Adana, F. Cátedra, and R. Mittra, "Incorporating the Multilevel Fast Multipole Method into the Characteristic Basis Function Method to solve large scattering and radiation problems," *IEEE AP-S International Symposium*, Honululu, Hawaii, pp. 1285-1288, June 2007.

[25] R. Maaskant, R. Mittra, and A. G. Tijhuis, "Fast analysis of large antenna arrays using the Characteristic Basis Function Method and the Adaptive Cross Approximation algorithm", *IEEE Trans. Antennas Propag*., vol. 56, no. 11, pp. 3440-3451, Nov. 2008.

[26] I. Stevanovic, and J. R. Mosig, "Subdomain multilevel approach with fast MBF interactions," *IEEE AP-S International Symposium*, Monterey, California, pp. 367-370, June 2004.

[27] P. De Vita, A. Freni, L. Matekovits, P. Pirinoli, and G. Vecchi, "A combined AIM-SFX approach for large complex arrays," IEEE AP-S International Symposium, Honulollu, Hawaii, pp. 3452-3455, June 2007.

[28] S. Rao, D. Wilton, and A. Glisson, "Electromagnetic scattering by surfaces of arbitrary shape," *IEEE Trans. Antennas Propag.*, vol. 30, no. 3, pp. 409-418, May 1982.

[29] G. H. Golub and C. F. van Loan, *Matrix Computation*, Baltimore, MD: John Hopkins Univ. Press, 1989.

[30] C. Delgado, F. Catedra, and R. Mittra, "A numerically efficient technique for orthogonalizing the basis functions arising in the solution of electromagnetic scattering problems using CBFM," *IEEE AP-S International Symposium*, Honulollu, Hawaii, pp. 3608-3611, June 2007.

[31] B. Delaunay, "Sur la sphère vide," *Izvestia Akademii Nauk SSSR, Otdelenie Matematicheskikh i Estestvennykh Nauk*, vol. 7, pp. 793-800, 1934.

[32] Personal communication with Prof. A. Boryssenko regarding the implementation of a MATLAB mesher, UMASS, 2004.

[33] A. K. Skriverik and J. R. Mosig, "Analysis of finite phase arrays of microstrip patches," *IEEE Trans. Antennas Propag*., vol. 41, no. 8, pp. 1105-1114, Aug. 1993.

[34] A. K. Skriverik, and J. R. Mosig, "Analysis of printed array antennas," *IEEE Trans. Antennas Propag.*, vol. 45, no. 9, pp. 1411-1418, Sept. 1997.

[35] C. Craeye, A. G. Tijhuis, and D. H. Schaubert, "An efficient mom formulation for finite-by-infinite arrays of two-dimensional antennas arranged in a three-dimensional structur," *IEEE Trans. Antennas Propag.*, vol. 51, no. 9, pp. 2054-2056, Sep. 2003.

[36] A. Neto, S. Maci, G. Vecchi, and M. Sabbadini, "A truncated floquet wave diffraction method for the full wave analysis of large phased arrays - part II: Generalization to 3-D cases," *IEEE Trans. Antennas Propag.*, vol. 48, no. 3, pp. 601-611, Mar. 2000.

[37] D. H. Schaubert, and A. O. Boryssenko, "Subarrays of Vivaldi antennas for very large apertures," *Proc. 34th European Microwave Conference*, Amsterdam, pp. 1533-1536, 2004.

[38] D. H. Schaubert, S. Kasturi, M. W. Elsallal, and W. van Cappellen, "Wide bandwidth Vivaldi antenna arrays - some recent developments," *Proc. European Conf. on Antennas and Propag*., Nice, France, 2006.

[39] R. Maaskant and B. Woestenburg, "Applying the Active Antenna Impedance to Achieve Noise Match in Receiving Array Antennas", *Antennas and Propagation Symposium*, Hawaii, USA, pp. 5889-5892, June 2007.

[40] C. Craeye, Personal communication.

Rob Maaskant received the M.Sc. degree (*cum laude*) in electrical engineering from the Eindhoven University of Technology, The Netherlands, in 2003. Since then, he has been an antenna research engineer at the Netherlands Foundation for Research in Astronomy (ASTRON) where his research is carried out in the framework of the Square Kilometre Array (SKA) radio telescope project. He is currently working toward the Ph.D. degree in the field of numerically efficient integral-equation techniques for large finite array antennas. Besides, his research includes the characterization and design of antenna array receiving systems.

Raj Mittra (S'54–M'57–SM'69–F'71–LF'96) is a Professor in the Electrical Engineering Department, Pennsylvania State University, University Park. He is also Director of the Electromagnetic Communication Laboratory, which is affiliated with the Communication and Space Sciences Laboratory of the Electrical Engineering Department. Prior to joining Penn State, he was a Professor in the Electrical and Computer Engineering Department, University of Illinois, Urbana-Champaign. He is President of RM Associates, State College, PA, a consulting organization that provides services to industrial and governmental organizations, both in the U.S. and abroad. He has published more than 700 technical papers and more than 30 books or book chapters on various topics related to electromagnetics, antennas, microwaves, and electronic packaging. He has received three patents on communication antennas. He has advised more than 85 Ph.D. students and about an equal number of M.S. students, and has mentored approximately 50 postdoctoral research associates and visiting scholars in the EMC Laboratory. Prof. Mittra received the Guggenheim Fellowship Award in 1965, the IEEE Centennial Medal in 1984, IEEE Millennium Medal in 2000, the IEEE/AP-S Distinguished Achievement Award, the AP-S Chen-To Tai Distinguished Educator Award in 2004, and the IEEE Electromagnetics Award in 2006. He is a past President of AP-S and was an Editor of the IEEE Transactions on Antennas and Propagation.

Anton G. Tijhuis (M'88) was born in Oosterhout N.B., The Netherlands, in 1952. He received the M.Sc. degree in theoretical physics from Utrecht University, Utrecht, The Netherlands, in 1976, and the Ph.D. degree (*cum laude*) from the Delft University of Technology, Delft, The Netherlands, in 1987. From 1976 to 1986 and 1986 to 1993, he was an Assistant and Associate Professor with the Laboratory of Electromagnetic Research, Faculty of Electrical Engineering, Delft University of Technology. In 1993, he became a Full Professor of electromagnetics with the Faculty of Electrical Engineering, Eindhoven University of Technology, Eindhoven, The Netherlands. He has been a Visiting Scientist with the University of Colorado at Boulder, the University of Granada, Granada, Spain, the University of Tel Aviv, Tel Aviv, Israel, and with McDonnell Douglas Research Laboratories, St. Louis, MO. Since 1996, he has been a Consultant with TNO Defence, Security, and Safety, The Hague, The Netherlands. His research interests are the analytical, numerical, and physical aspects of the theory of electromagnetic waves. In particular, he is involved with efficient techniques for the computational modeling of electromagnetic fields and their application to detection and synthesis problems from several areas of electrical engineering.